THE JOURNAL OF PHYSICAL CHEMISTRY Letters

Letter

pubs.acs.org/JPCL

Depth-Dependent Heterogeneity in Membranes by Fluorescence Lifetime Distribution Analysis

Sourav Haldar,[†] Mamata Kombrabail,[§] G. Krishnamoorthy,[§] and Amitabha Chattopadhyay*,[†]

[†]Centre for Cellular and Molecular Biology, Council of Scientific and Industrial Research, Uppal Road, Hyderabad 500 007, India

[§]Department of Chemical Sciences, Tata Institute of Fundamental Research, Homi Bhabha Road, Mumbai 400 005, India

ABSTRACT: Biological membranes display considerable anisotropy due to differences in composition, physical characteristics, and packing of membrane components. In this Letter, we have demonstrated the environmental heterogeneity along the bilayer normal in a depth-dependent manner using a number of anthroyloxy fatty acid probes. We employed fluorescence lifetime distribution analysis utilizing the maximum entropy method (MEM) to assess heterogeneity. Our results show that the fluorescence lifetime heterogeneity varies considerably depending on fluorophore location along the membrane normal (depth), and it is the result of the anisotropic environmental heterogeneity along the bilayer normal. Environmental heterogeneity is reduced as the reporter group is moved from the membrane interface to a deeper hydrocarbon region. To the best of our knowledge, our results constitute the first experimental demonstration of anisotropic heterogeneity in bilayers. We conclude that such graded environmental heterogeneity represents an intrinsic characteristics of the membrane bilayer and envisage that it has a role in the conformation and orientation of membrane proteins and their function.

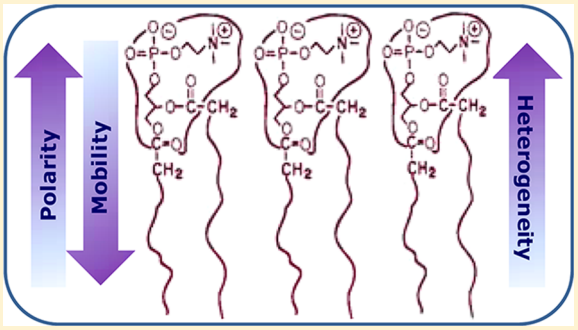

SECTION: Biophysical Chemistry and Biomolecules

Biological membranes are highly organized, complex, noncovalent molecular assemblies of lipids and proteins that allow cellular compartmentalization and act as a physical prerequisite for natural evolution.[1] Membranes therefore provide cells with the much needed identity. They act as the interface through which cells communicate with each other and with the external milieu. Membranes represent an ideal environment for the proper function of membrane proteins and constitute the site of many important cellular functions.

A fascinating aspect of biological membranes is the intrinsic anisotropy along the axis perpendicular to the membrane plane.[2−4] Although the center of the bilayer is almost isotropic, the upper region, only a few angstroms away toward the membrane surface, is highly ordered. As a result, properties such as polarity, order (fluidity), segmental motion, ability to form hydrogen bonds, and extent of solvent penetration vary in a depth-dependent fashion along the *z*-axis of the membrane. A consequence of such an anisotropic environment is the differential extents to which the mobility of solvent (water) molecules are retarded at different depths in the membrane relative to their mobility in the bulk aqueous phase.[5]

Considerable evidence shows that biological membranes exhibit lateral (conformational) heterogeneity in terms of the composition of membrane components, physical properties such as order, and lipid packing (compactness).[6] Heterogeneity could be manifested as both spatial and temporal domains.[7] For example, cholesterol is known to influence membrane heterogeneity.[6,8] Interestingly, although there are a number of spectroscopic and computational approaches to monitor membrane order, there are relatively few techniques available to assess heterogeneity. Approaches based on NMR, differential scanning calorimetry, and X-ray crystallography are not suitable for measurement of membrane heterogeneity. Analysis of fluorescence lifetime distribution of membrane probes have proved to be useful for monitoring structural and dynamic heterogeneity in membranes.[9−14] Although lateral heterogeneity in membranes has been explored extensively using fluorescence spectroscopy and microscopy due to various types of domain formation,[7,8] variation in the extent of lateral heterogeneity along the membrane normal remains a less explored topic.[15]

In this Letter, we have demonstrated the environmental heterogeneity along the bilayer normal in a depth-dependent manner in the membrane bilayer. For this purpose, we used fluorescence lifetime distribution analysis of *n*-(9-anthroyloxy)-stearic acid (*n*-AS, where *n* is the position of the carbon atom where the anthroyloxy group is attached; see Figure 1) probes utilizing the maximum entropy method (MEM). Anthroyloxy fatty acids with the anthroyloxy group covalently attached to different positions of the fatty acyl chain represent a unique set of reporter molecules with a common fluorophore attached at different positions along the bilayer normal. These probes have

Received: August 24, 2012
Accepted: September 4, 2012
Published: September 4, 2012

   dx.doi.org/10.1021/jz3012589 | *J. Phys. Chem. Lett.* 2012, 3, 2676−2681

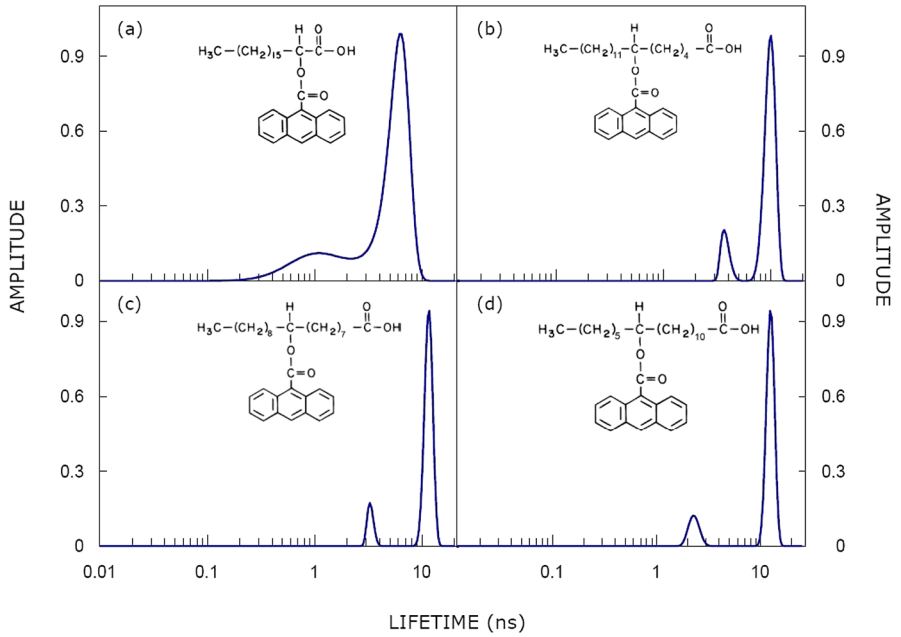

Figure 1. MEM lifetime distribution of AS probes in DOPC membranes for (a) 2-AS, (b) 6-AS, (c) 9-AS, and (d) 12-AS. The structures of the AS probes are also shown. The ratio of probe to DOPC was 1:100 (mol/mol), and the concentration of DOPC was 0.47 mM. See the Experimental Section for other details.

been found to be located at a graded series of depths in the membrane bilayer, depending on the position of the attachment of the anthroyloxy group to the fatty acyl chain.[16−18] We show here that the heterogeneity in the bilayer is dependent on the position of the reporter (anthroyloxy) group in the *z*-axis, thereby setting up a natural gradient of heterogeneity along the bilayer normal. Consistent with the anisotropic nature of the membrane bilayer, the degree of heterogeneity exhibits a reduction as the reporter group is moved away from the membrane interface to a deeper hydrocarbon region.

Fatty acids labeled with fluorescent groups have proved to be useful membrane probes.[19] Anthroyloxy fatty acids in which an anthracene group is attached by an ester linkage to various positions of an alkyl chain have been extensively used as fluorescent probes in membranes and membrane-mimetic media.[5,16,20−25] It has been previously shown that the depth of the anthroyloxy group is almost linearly related to the number of carbon atoms between it and the carboxyl group (this is not true for other membrane probes such as the NBD probes, which often loop back to the membrane interface[26−29]).[18] Depth analysis using the parallax method[26] has previously shown that the anthroyloxy probes used in this work (see Figure 1 for chemical structures of AS probes) are localized at progressively increasing depths as the site of attachment of the anthroyloxy group is moved (from C-2 to C-12) along the acyl chain of the fatty acid. The depths of the anthroyloxy group have been determined to be 15.8, 12.3, 8.8, and 6 Å from the center of the bilayer for 2-AS, 6-AS, 9-AS, and 12-AS, respectively, at pH 5 (see Table 1).[18] Taken together, these AS probes represent a set of depth markers.

The anthroyloxy group displays a large change in dipole moment upon excitation[30] that results in a large Stokes' shift[31] and makes fluorescence of AS probes sensitive to the immediate environment. Fluorescence lifetime serves as a sensitive indicator of the local environment and polarity in which a given fluorophore is localized.[32] Table 1 shows lifetimes of AS probes in DOPC membranes analyzed by the discrete analysis method. As apparent from the table, all fluorescence decays could be fitted well with a biexponential function. The amplitude-averaged lifetimes (τ_m) and intensity-averaged lifetimes ($\langle\tau\rangle$) of AS probes were calculated using eqs 2 and 3 and are shown in Table 1. Interestingly, both τ_m and $\langle\tau\rangle$ exhibit a depth-dependent increase as follows: 2-AS < 6-AS < 9-AS < 12-AS. The longest fluorescence lifetime is displayed by 12-AS (the deepest probe). On the other hand, 2-AS (the most shallow probe) exhibits the shortest lifetime. The lifetimes of 6- and 9-AS are intermediate between these two extreme values. We interpret the increase in fluorescence lifetime with membrane penetration depth due to the concomitant reduction in environmental polarity along the bilayer normal.[2] It has previously been shown that fluorescence lifetime of AS probes depends on the polarity of the medium.[21]

Table 1. Representative Fluorescence Lifetimes of AS Probes[a]

probe	α_1	τ_1 (ns)	α_2	τ_2 (ns)	τ_m (ns)[c]	$\langle\tau\rangle$ (ns)[d]
2-AS (15.8 Å)[b]	0.19	1.96	0.81	6.60	5.72	6.30
6-AS (12.3 Å)	0.11	2.21	0.89	8.87	8.14	8.68
9-AS (8.8 Å)	0.09	2.21	0.91	11.47	10.64	11.30
12-AS (6 Å)	0.19	3.01	0.81	12.72	10.88	12.21

[a]The excitation wavelength was 366 nm, and emission was monitored at 460 nm. All other conditions are as in Figure 1. The errors were 5−10% for all parameters. See the Experimental Section for other details. [b]The numbers in parentheses indicate the depth of the anthroyloxy group from the center of the bilayer (from ref 18). [c]Calculated using eq 5. [d]Calculated using eq 6.

Fluorescence decay kinetics of probes incorporated in complex microheterogeneous systems generally displays a considerable level of heterogeneity. The lifetime distribution of fluorescent probes in these cases represents a powerful method for characterizing complex systems such as membranes. The width of the lifetime distribution can be effectively utilized to interpret the degree of heterogeneity of membranes and

dx.doi.org/10.1021/jz3012589 | J. Phys. Chem. Lett. 2012, 3, 2676−2681

membrane proteins.[8,13,33] Fluorescence lifetime distribution analysis by the MEM represents a convenient, robust, and model-free approach of data analysis.[34−36] In the MEM approach, the fluorescence intensity decay ($I(t)$) is analyzed using the model of continuous distribution of lifetimes

$$I(t) = \int_0^\infty \alpha(\tau) \exp(-t/\tau)\, d\tau \quad (1)$$

where $\alpha(\tau)$ represents the amplitude corresponding to the lifetime τ in the intensity decay. The limits on the above integration are generally set based on the information regarding the system under study and the detection limit of the instrument. We set the lower and the upper limits of the integration as 10 ps and 20 ns, respectively. For practical reasons, the above equation can be written in terms of a discrete sum of exponentials as

$$I(t) = \sum_{i=1}^{N} \alpha_i \exp(-t/\tau_i) \quad (2)$$

where N represents the total number of exponentials. In our analysis, N is taken as 100 exponentials equally spaced in the $\log(\tau)$ space between the lower and upper limits. MEM initially starts with a flat distribution of amplitudes $\alpha(\tau)$, that is, assuming that each lifetime has equal contribution in the beginning and arrives at the amplitude distribution that best describes the observed experimental fluorescence intensity decay. The optimization of the amplitude distribution $\alpha(\tau)$ is carried out in successive cycles by minimizing the χ^2 value (close to 1 in all cases) and maximizing the entropy (S).[34] The expression used for S is the Shannon−Jayne's entropy function, expressed as

$$S = -\sum p_i \log p_i \qquad \text{where} \quad p_i = \frac{\alpha_i}{\sum \alpha_i} \quad (3)$$

Successive iterations provide a distribution that minimizes χ^2 and maximizes S. If the χ^2 criterion is satisfied by many distributions in a particular iteration, then the distribution with maximum entropy is selected. The analysis is terminated when χ^2 reaches the specified lower limit or when χ^2 and $\alpha(\tau)$ show no change in successive iterations. Importantly, MEM analysis gives a lifetime distribution that is model-independent.

Figure 1 shows the representative lifetime distribution obtained by MEM analysis of AS probes in DOPC membranes. Interestingly, the lifetime distribution profile of AS probes exhibits a marked dependence on the position of the anthroyloxy probe in the fatty acyl chain. The lifetime distribution appears to be sharper for probes that are localized deeper in the membrane bilayer. The widths of the fluorescence lifetime distribution, represented as full width at half-maxima (FWHM) for the major peak, for AS probes as a function of depth in the membrane are shown in Figure 2.

The FWHM for the shallow probe 2-AS is 2.72 ns, while that for the probe localized deepest in the membrane (12-AS) is 1.97 ns. This difference in FWHM is indicative of the contrasting heterogeneity experienced by the anthroyloxy groups in these two locations in the membrane. The reason for such location-specific membrane heterogeneity lies in the intrinsic anisotropy along the axis perpendicular to the membrane plane.[2−4] The FWHM values for the other probes, 6- and 9-AS, are intermediate between these two values. Interestingly, Figure 2 shows that there is a sharp change in the width (FWHM) of the lifetime distribution between 2-AS and

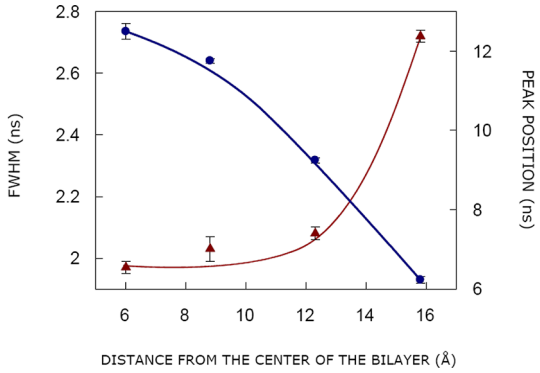

Figure 2. Variation of the width of the fluorescence lifetime distribution (represented as the FWHM; ▲, maroon) and the position of the major peak (●, blue) as a function of the distance of the anthroyloxy group from the center of the bilayer (depth). Depth values of AS probes were obtained from ref 18. Lines joining the data points are provided merely as viewing guides. Data represent means ± SE of at least three independent measurements. See the Experimental Section for other details.

6-AS that is followed by a more gradual reduction in FWHM. This could be due to the drastic change in environment immediately below the interfacial region where 6-AS is localized. The position of the major peak of the lifetime distribution, on the other hand, displays an opposite trend (i.e., highest for the deep probe 12-AS and lowest for the shallow probe 2-AS; see Figure 2) due to the reduction in environmental polarity along the bilayer normal.

MEM represents an unbiased (model-free) and robust approach for analyzing the fluorescence lifetime distribution.[34−36] The width (FWHM) of the lifetime distribution obtained by this method is correlated with the degree of environmental heterogeneity as sensed by the fluorophore.[8,13,33] Our results show that the environmental heterogeneity experienced by the anthroyloxy group varies considerably depending on its location along the membrane normal (depth). The shallow probe 2-AS localized at the membrane interface experiences considerable heterogeneity, as is evident from a FWHM value of 2.72 ns (Figures 2 and 3).

The membrane interfacial region is characterized by unique motional and dielectric characteristics[37] different from those of the bulk aqueous phase and the more isotropic hydrocarbon-like deeper regions of the membrane. The confined water molecules at the membrane interface become ordered due to the reduced possibility of energetically favorable hydrogen bonding arising out of geometrical constraints.[38] The interfacial region of the membrane exhibits slow rates of solvent relaxation[5] and is also known to participate in intermolecular charge interactions[39] and hydrogen bonding through the polar lipid headgroup.[40,41] These features of the membrane interfacial region contribute to environmental heterogeneity, as experienced by 2-AS. In contrast to this, the anthroyloxy group in 12-AS is localized in the deep hydrocarbon-like more isotropic environment that is less restrictive (which allows more "sampling", thereby reducing heterogeneity). This results in 12-AS experiencing a relatively less heterogeneous environment, apparent from its FWHM value (Figures 2 and 3).

We believe that this trend of width and peak position of the lifetime distribution is a manifestation of the intrinsic anisotropy in environmental heterogeneity, characteristic of membrane bilayers (see Figure 3). In other words, the

dx.doi.org/10.1021/jz3012589 | J. Phys. Chem. Lett. 2012, 3, 2676−2681

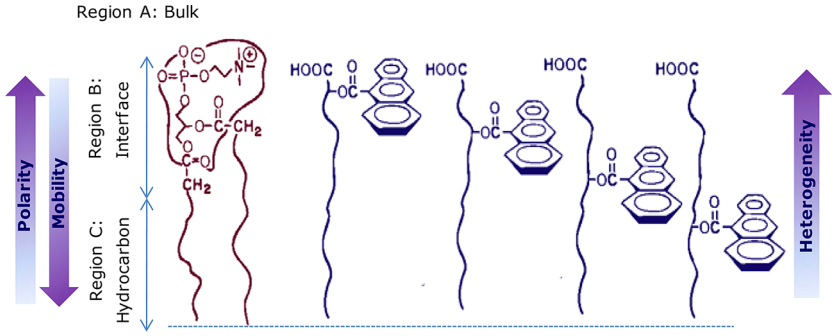

Figure 3. A schematic representation of half of the membrane bilayer showing the localizations of the anthroyloxy groups in AS probes. The horizontal line at the bottom indicates the center of the bilayer. The membrane anisotropy along the axis perpendicular to the plane of the bilayer divides the membrane leaflet into three broad regions exhibiting very different composition and dynamics, Region A: bulk aqueous phase characterized by fast solvent relaxation; Region B: membrane interface characterized by slow (restricted) solvent relaxation, hydrogen bonding (important for functionality), water penetration (interfacial water), and high anisotropy; Region C: bulk hydrocarbon-like environment, isotropic, fast solvent relaxation. The arrows along the membrane perpendicular (*z*-axis) indicate gradients in polarity, mobility, and heterogeneity along the bilayer normal. Adapted and modified from refs 4 and 5.

environmental heterogeneity is the different physicochemical environment sampled at different depths in the membrane due to the difference in composition and dynamics along the bilayer normal (shown in Figure 3). As a consequence of this, the degree of in-plane heterogeneity is critically dependent on the localization (depth) of the probe, giving rise to anisotropic heterogeneity. In a broader context, such anisotropy allows proper functioning of membrane proteins. The biological membrane provides a unique environment to membrane-spanning proteins and peptides, thereby influencing their structure and function. Membrane-spanning proteins have distinct stretches of hydrophobic amino acids that form the membrane-spanning domain, and the distribution of amino acids along the membrane normal appear asymmetric. For example, tryptophan residues in integral membrane proteins and peptides are not uniformly distributed, and they tend to be localized toward the membrane interface, possibly because they are involved in hydrogen bonding[42] with the lipid carbonyl groups or interfacial water molecules. It is for this reason that it has been recently suggested that the physical properties of the membrane bilayer in which a protein will reside impose constraints on the composition and sequence of the transmembrane domain(s) of the protein.[43] This explains the organelle specificity displayed by transmembrane domains of membrane proteins. In summary, our results demonstrate the existence of an anisotropic environmental heterogeneity along the bilayer normal, in addition to the polarity and mobility gradient.[2−5]

■ EXPERIMENTAL SECTION

1,2-Dioleoyl-*sn*-glycero-3-phosphocholine (DOPC) was obtained from Avanti Polar Lipids (Alabaster, AL). 1,2-Dimyristoyl-*sn*-glycero-3-phosphocholine (DMPC) and sodium acetate were obtained from Sigma Chemical Co. (St. Louis, MO). *n*-AS probes (2-, 6-, 9- and 12-(9-anthroyloxy)stearic acid) were from Molecular Probes (Eugene, OR). DOPC was checked for purity by thin-layer chromatography on silica gel precoated plates (Sigma) in chloroform/methanol/water (65:35:5, v/v/v) and was found to give only one spot with a phosphate-sensitive spray and upon subsequent charring.[44] Concentrations of stock solutions of *n*-AS probes in methanol were estimated using the molar extinction coefficient (ε) of 8000 M^{-1} cm^{-1} at 361 nm.[45] The concentration of DOPC was determined by phosphate assay subsequent to total digestion by perchloric acid.[46] DMPC was used as an internal standard to assess lipid digestion. Solvents used were of spectroscopic grade. Water was purified through a Millipore (Bedford, MA) Milli Q system and used throughout. Unilamellar vesicles (ULV) of DOPC labeled with 1% (mol/mol) of one of the AS probes were prepared by the ethanol injection method.[47] This method produces predominantly unilamellar vesicles of ∼100 nm diameter. For this, 640 nmol of DOPC and 6.4 nmol of the fluorescent probe were dried together. The dried lipids were then dissolved in ethanol to give a final concentration of 40 mM. This ethanolic lipid solution was then injected into 10 mM sodium acetate, 150 mM sodium chloride, pH 5 buffer while vortexing to give a final concentration of 0.47 mM lipid in the buffer. Experiments were carried out at pH 5 so that the anthroyloxy probes were in their protonated states and ground-state heterogeneity due to partial ionization of the carboxyl group was avoided.[48] All experiments were carried out at room temperature (∼23 °C), where DOPC exists in the fluid phase. Time-resolved fluorescence intensity decay measurements were carried out using a time-correlated single-photon counting (TCSPC) setup. For fluorescence lifetime measurements, 1 ps pulses of 732 nm radiation from the Ti-sapphire femto/picosecond laser (Spectra Physics, Mountain View, CA), pumped by a Nd:YLF laser (Millenia X, Spectra Physics), were frequency-doubled to 366 nm by using a frequency doubler/tripler (GWU, Spectra Physics). Fluorescence decay curves were obtained at the laser repetition rate of 4 MHz by a microchannel plate photomultiplier (model R2809u, Hamamatsu Corp.) coupled to a TCSPC setup. The instrument response function (IRF) at 366 nm was obtained using a dilute colloidal suspension of dried nondairy creamer. The full width at half-maximum (FWHM) of the IRF was 40 ps, and the number of channels used was 1024. Fluorescence emission measurements of AS probes, excited at 366 nm, were carried out at 460 nm, using a combination of a monochromator and a 400 nm cutoff filter. Fluorescence intensity decay was collected from the sample after excitation with the emission polarizer oriented at the magic angle (54.7°) with respect to the excitation polarizer. The fluorescence emission at the magic angle (54.7°) was dispersed in a monochromator (spectral width 2.5 nm), counted ($(3-4) \times 10^3$ s^{-1}) by a microchannel plate photomultiplier, and processed through a constant

dx.doi.org/10.1021/jz3012589 | *J. Phys. Chem. Lett.* 2012, 3, 2676−2681

fraction discriminator, time-to-amplitude converter, and multichannel analyzer. To optimize the signal-to-noise ratio, 20 000 photon counts were collected in the peak channel. All experiments were performed using excitation and emission slits with a nominal bandpass of 3 nm or less. The data stored in the multichannel analyzer were routinely transferred to an IBM PC for analysis. Additional details of TCSPC measurements are provided in refs 8 and 33. Fluorescence intensity decay curves so obtained were deconvoluted with the instrument response function and analyzed as a sum of exponential terms

$$F(t) = \sum_i \alpha_i \exp(-t/\tau_i) \tag{4}$$

where $F(t)$ is the fluorescence intensity at time t and α_i is a preexponential factor representing the fractional contribution to the time-resolved decay of the component with a lifetime τ_i such that $\sum_i \alpha_i = 1$. The decay parameters were recovered using a nonlinear least-squares iterative fitting procedure based on the Levenberg–Marquardt algorithm.[49,50] A fit was considered acceptable when plots of the weighted residuals and the autocorrelation function showed random deviation about zero with a minimum χ^2 value not more than 1.2. Fluorescence decays were analyzed by the discrete exponential analysis as well as the maximum entropy method (MEM). Amplitude-averaged lifetimes (τ_m) and intensity-averaged lifetimes ($\langle\tau\rangle$) for biexponential decays of fluorescence were calculated from the decay times and preexponential factors using the following equations[51,52]

$$\tau_m = \alpha_1\tau_1 + \alpha_2\tau_2 \tag{5}$$

$$\langle\tau\rangle = \frac{\alpha_1\tau_1^2 + \alpha_2\tau_2^2}{\alpha_1\tau_1 + \alpha_2\tau_2} \tag{6}$$

AUTHOR INFORMATION

Corresponding Author

*Tel.: +91-40-2719-2578. Fax: +91-40-2716-0311. E-mail: amit@ccmb.res.in.

Notes

The authors declare no competing financial interest.

ACKNOWLEDGMENTS

This work was supported by the Council of Scientific and Industrial Research (A.C.) and Department of Atomic Energy (G.K.), Govt. of India. S.H. thanks the Council of Scientific and Industrial Research for the award of a Senior Research Fellowship. A.C. is an Adjunct Professor at the Special Centre for Molecular Medicine of Jawaharlal Nehru University (New Delhi, India) and Indian Institute of Science Education and Research (Mohali, India) and Honorary Professor at the Jawaharlal Nehru Centre for Advanced Scientific Research (Bangalore, India). A.C. and G.K. gratefully acknowledge J.C. Bose Fellowship (Department of Science and Technology, Govt. of India). We thank Prof. N. Periasamy (TIFR, Mumbai, India) for providing the software for the analysis of MEM data. We thank Saswata Sarkar for helpful discussions and members of A.C.'s research group for critically reading the manuscript.

REFERENCES

(1) Budin, I.; Szostak, J. W. Expanding Roles for Diverse Physical Phenomena During the Origin of Life. *Annu. Rev. Biophys.* **2010**, *39*, 245–263.

(2) Stubbs, C. D.; Ho, C.; Slater, S. J. Fluorescence Techniques for Probing Water Penetration into Lipid Bilayers. *J. Fluoresc.* **1995**, *5*, 19–28.

(3) Chattopadhyay, A. Exploring Membrane Organization and Dynamics by the Wavelength-Selective Fluorescence Approach. *Chem. Phys. Lipids* **2003**, *122*, 3–17.

(4) Haldar, S.; Chaudhuri, A.; Chattopadhyay, A. Organization and Dynamics of Membrane Probes and Proteins utilizing the Red Edge Excitation Shift. *J. Phys. Chem. B* **2011**, *115*, 5693–5706.

(5) Chattopadhyay, A.; Mukherjee, S. Depth-Dependent Solvent Relaxation in Membranes: Wavelength-Selective Fluorescence as a Membrane Dipstick. *Langmuir* **1999**, *15*, 2142–2148.

(6) Falck, E.; Patra, M.; Karttunen, M.; Hyvönen, M. T.; Vattulainen, I. Impact of Cholesterol on Voids in Phospholipid Membranes. *J. Chem. Phys.* **2004**, *121*, 12676–12689.

(7) Mukherjee, S.; Maxfield, F. R. Membrane Domains. *Annu. Rev. Cell Dev. Biol.* **2004**, *20*, 839–866.

(8) Mukhejee, S.; Kombrabail, M.; Krishnamoorthy, G.; Chattoapadhyay, A. Dynamics and Heterogeneity of Bovine Hippocampal Membranes: Role of Cholesterol and proteins. *Biochim. Biophys. Acta* **2007**, *1768*, 2130–2144.

(9) Williams, B. W.; Stubbs, C. D. Properties Influencing Fluorophore Lifetime Distributions in Lipid Bilayers. *Biochemistry* **1988**, *27*, 7994–7999.

(10) Stubbs, C. D.; Williams, B. W.; Ho, C. Fluorophore Lifetime Distributions as a Probe of Lipid Bilayer Organization. *Proc. SPIE* **1990**, *1204*, 448–455.

(11) Ho, C.; Williams, B. W.; Kelly, M. B.; Stubbs, C. D. Chronic Ethanol Intoxication Induces Adaptive Changes at the Membrane Protein/Lipid Interface. *Biochim. Biophys. Acta* **1994**, *1189*, 135–142.

(12) Davenport, L. Fluorescence Probes for Studying Membrane Heterogeneity. *Methods Enzymol.* **1997**, *278*, 487–512.

(13) Krishnamoorthy, G.; Ira. Fluorescence Lifetime Distribution in Characterizing Membrane Microheterogeneity. *J. Fluoresc.* **2001**, *11*, 247–253.

(14) Krishnamoorthy, G.; Srivastava, A. Intracellular Dynamics Seen Through Time-Resolved Fluorescence Microscopy. *Curr. Sci.* **1997**, *72*, 835–855.

(15) Mazor, S.; Vanounou, S.; Fishov, I. Pyrene as a Membrane Depth Gauge: Wavelength Selective Fluorescence Approach to Monitor Pyrene Localizations in the Membrane. *Chem. Phys. Lipids* **2012**, *165*, 125–131.

(16) Villalain, J.; Prieto, M. Location and Interaction of N-(9-anthroyloxy)-stearic Acid Probes Incorporated in Phosphatidylcholine Vesicles. *Chem. Phys. Lipids* **1991**, *59*, 9–16.

(17) Abrams, F. S.; Chattopadhyay, A.; London, E. Determination of the Location of Fluorescent Probes Attached to Fatty Acids State and Environment on Depth using Parallax Analysis of Fluorescence Quenching: Effect of Carboxyl Ionization. *Biochemistry* **1992**, *31*, 5322–5327.

(18) Abrams, F. S.; London, E. Extension of the Parallax Analysis of Membrane Penetration Depth to the Polar Region of Model Membranes: Use of Fluorescence Quenching by a Spin-Label Attached to the Phospholipid Polar Headgroup. *Biochemistry* **1993**, *32*, 10826–10831.

(19) Lala, A. K.; Koppaka, V. Fluorenyl Fatty Acids as Fluorescent Probes for Depth-Dependent Analysis of Artificial and Natural Membranes. *Biochemistry* **1992**, *31*, 5586–5593.

(20) Tilley, L.; Thulborn, K. R.; Sawyer, W. H. An Assessment of the Fluidity Gradient of the Lipid Bilayer as Determined by a Set of n-(9-Anthroyloxy) Fatty Acids (n = 2, 6, 9, 12, 16). *J. Biol. Chem.* **1979**, *254*, 2592–2594.

(21) Thulborn, K. R.; Tilley, L. M.; Sawyer, W. H.; Treloar, F. E. The use of n-(9-Anthroyloxy) Fatty Acids to Determine Fluidity and

Polarity Gradients in Phospholipid Bilayers. *Biochim. Biophys. Acta* **1979**, *558*, 166−178.
(22) Hutterer, R.; Schneider, F. W.; Lanig, H.; Hof, M. Solvent Relaxation Behaviour of n-Anthroyloxy Fatty Acids in PC-Vesicles and Paraffin Oil: A Time-Resolved Emission Spectra Study. *Biochim. Biophys. Acta* **1997**, *1323*, 195−207.
(23) Kelkar, D. A.; Ghosh, A.; Chattopadhyay, A. Modulation of Fluorophore Environment in Host Membranes of Varying Charge. *J. Fluoresc.* **2003**, *13*, 459−466.
(24) Kelkar, D. A.; Chattopadhyay, A. Depth-Dependent Solvent Relaxation in Reverse Micelles: A Fluorescence Approach. *J. Phys. Chem. B* **2004**, *108*, 12151−12158.
(25) Mukherjee, S.; Chattopadhyay, A. Influence of Ester and Ether Linkage in Phospholipids on the Environment and Dynamics of the Membrane Interface: A Wavelength-Selective Fluorescence Approach. *Langmuir* **2005**, *21*, 287−293.
(26) Chattopadhyay, A.; London, E. Parallax Method for Direct Measurement of Membrane Penetration Depth Utilizing Fluorescence Quenching by Spin-Labeled Phospholipids. *Biochemistry* **1987**, *26*, 39−45.
(27) Chattopadhyay, A.; London, E. Spectroscopic and Ionization Properties of N-(7-Nitrobenz-2-oxa-1,3-diazol-4-yl)-Labeled Lipids in Model Membranes. *Biochim. Biophys. Acta* **1988**, *938*, 24−34.
(28) Mukherjee, S.; Raghuraman, H.; Dasgupta, S.; Chattopadhyay, A. Organization and Dynamics of N-(7-Nitrobenz-2-oxa-1,3-diazol-4-yl)-Labeled Lipids: A Fluorescence Approach. *Chem. Phys. Lipids* **2004**, *127*, 91−101.
(29) Raghuraman, H.; Shrivastava, S.; Chattopadhyay, A. Monitoring the Looping up of Acyl Chain Labeled NBD Lipids in Membranes as a Function of Membrane Phase State. *Biochim. Biophys. Acta* **2007**, *1768*, 1258−1267.
(30) Werner, T. C.; Hoffman, R. M. Relation Between an Excited State Geometry Change and the Solvent Dependence of 9-Methyl Anthroate Fluorescence. *J. Phys. Chem.* **1973**, *77*, 1611−1615.
(31) Garrison, M. D.; Doh, L. M.; Potts, R. O.; Abraham, W. Fluorescence Spectroscopy of 9-Anthroyloxy Fatty Acids in Solvents. *Chem. Phys. Lipids* **1994**, *70*, 155−162.
(32) Prendergast, F. G. Time-Resolved Fluorescence Techniques: Methods and Applications in Biology. *Curr. Opin. Struct. Biol.* **1991**, *1*, 1054−1059.
(33) Haldar, S.; Kombrabail, M.; Krishnamoorthy, G.; Chattopadhyay, A. Monitoring Membrane Protein Conformational Heterogeneity by Fluorescence Lifetime Distribution Analysis using the Maximum Entropy Method. *J. Fluoresc.* **2010**, *20*, 407−413.
(34) Brochon, J. C. Maximum Entropy Method of Data Analysis in Time-Resolved Spectroscopy. *Methods Enzymol.* **1994**, *240*, 262−311.
(35) Swaminathan, R.; Krishnamoorthy, G.; Periasamy, N. Similarity of Fluorescence Lifetime Distributions for Single Tryptophan Proteins in the Random Coil State. *Biophys. J.* **1994**, *67*, 2013−2023.
(36) Swaminathan, R.; Periasamy, N. Analysis of Fluorescence Decay by the Maximum Entropy Method: Influence of Noise and Analysis Parameters on the Width of the Distribution of Lifetimes. *Proc. Indian Acad. Sci., Chem. Sci.* **1996**, *108*, 39−49.
(37) Ashcroft, R. G.; Coster, H. G. L.; Smith, J. R. The Molecular Organization of Bimolecular Lipid Membranes: The Dielectric Structure of the Hydrophilic/Hydrophobic Interface. *Biochim. Biophys. Acta* **1981**, *643*, 191−204.
(38) Marrink, S.-J.; Tielman, D. P.; van Buuren, A. R.; Berendsen, H. J. C. M. Membranes and Water: An Interesting Relationship. *Faraday Discuss.* **1996**, *103*, 191−201.
(39) Yeagle, P. *The Membranes of Cells*; Academic Press: Orlando, FL, 1987; pp 89−90.
(40) Boggs, J. M. Lipid Intermolecular Hydrogen Bonding: Influence on Structural Organization and Membrane Function. *Biochim. Biophys. Acta* **1987**, *906*, 353−404.
(41) Shin, T. B.; Leventis, R.; Silvius, J. R. Partitioning of Fluorescent Phospholipid Probes Between Different Bilayer Environments. Estimation of the Free Energy of Interlipid Hydrogen Bonding. *Biochemistry* **1991**, *30*, 7491−7497.
(42) Ippolito, J. A.; Alexander, R. S.; Christianson, D. W. Hydrogen Bond Stereochemistry in Protein Structure and Function. *J. Mol. Biol.* **1990**, *215*, 457−471.
(43) Sharpe, H. J.; Stevens, T. J.; Munro, S. A Comprehensive Comparison of Transmembrane Domains Reveals Organelle-Specific Properties. *Cell* **2010**, *142*, 158−169.
(44) Baron, C. B.; Coburn, R. F. Comparison of Two Copper Reagents for Detection of Saturated and Unsaturated Neutral Lipids by Charring Densitometry. *J. Liq. Chromatogr.* **1984**, *7*, 2793−2801.
(45) Haugland, R. P. *Handbook of Fluorescent Probes and Research Chemicals*, 6th ed.; Molecular Probes Inc: Eugene, OR, 1996.
(46) McClare, C. W. F. An Accurate and Convenient Organic Phosphorus Assay. *Anal. Biochem.* **1971**, *39*, 527−530.
(47) Kremer, J. M. H.; Esker, M. W. J.; Pathmamanoharan, C.; Wiersema, P. H. Vesicles of Variable Diameter Prepared by a Modified Injection Method. *Biochemistry* **1977**, *16*, 3932−3935.
(48) Von Tscharner, V.; Radda, G. K. The Effect of Fatty Acids on the Surface Potential of Phospholipid Vesicles Measured by Condensed Phase Radioluminescence. *Biochim. Biophys. Acta* **1981**, *643*, 435−448.
(49) Bevington, P. R. *Data Reduction and Error Analysis for the Physical Sciences*; McGraw-Hill: New York, 1969.
(50) O'Connor, D. V.; Phillips, D. *Time-Correlated Single Photon Counting*; Academic Press: London, 1984; pp 180−189.
(51) Valeur, B. *Molecular Fluorescence*; Wiley-VCH: Weinheim, Germany, 2002.
(52) Lakowicz, J. R. *Principles of Fluorescence Spectroscopy*, 3rd ed.; Springer: New York, 2006.